



ARTICLE

Investigation of the Interaction Mechanism between Lignin Structural Units and Enzyme

Lijing Huang, Penghui Li, Kangjie Jiang and Wenjuan Wu*

Jiangsu Co-Innovation Center of Efficient Processing and Utilization of Forest Resources, Nanjing Forestry University, Nanjing, 210037, China

*Corresponding Author: Wenjuan Wu. Email: wenjuanwu@njfu.edu.cn

Received: 05 May 2022 Accepted: 01 July 2022

ABSTRACT

The effect of lignin structural units on enzymatic hydrolysis of lignocellulosic biomass was investigated, especially the inhibitory role of lignin in non-productive adsorption with enzymes. Milled wood lignin (MWL) was isolated from different hardwoods of poplar, eucalyptus and acacia. The isolated lignin samples were characterized by elemental analysis, gel permeation chromatography, nitrobenzene oxidation and fourier infrared spectroscopy. The mechanism of lignin structural units on enzymatic hydrolysis of cellulose was studied by quartz crystal microbalance (QCM). The results showed that different structural units of lignin had different adsorption capacity for enzymes. The results of nitrobenzene oxidation indicated that the S/G ratio (S: syringyl-like lignin structures; G: guaiacyl-like lignin structures) of lignin of poplar was 0.99, that of eucalyptus was 1.92 and that of acacia was 1.34. According to the results of QCM, the adsorption capacity of the three lignin films was as follows: Poplar MWL (S/G ratio 0.99) < Acacia MWL (S/G ratio 1.34) < Eucalyptus MWL (S/G ratio 1.92). Eucalyptus MWL with higher degree of condensation and S/G ratio showed stronger affinity to enzymes and more non-productive adsorption with enzymes, resulting in less adsorption between enzymes and cellulose, and lower enzymatic hydrolysis efficiency.

KEYWORDS

Lignin; structural unit; enzyme adsorption; enzymatic hydrolysis

1 Introduction

With the development of industrialization and the growth of population, energy consumption has increased significantly, and fossil fuel reserves can not meet the growing energy demand. Most important of all, fossil fuel is unsustainable, which brings many environmental pollution problems, such as sulfur dioxide and nitrogen dioxide produced from burning [1]. Therefore, the focus of energy research began to shift to bioenergy which can replace fossil fuel, mainly because bioenergy sources are clean available and have a wide range of raw materials, including bioethanol, biomethane and bio-oil [2]. Using lignocellulosic materials to produce bioethanol is conducive to reducing the dependence on fossil fuel, alleviating energy pressure, and helping to achieve “peak carbon dioxide emissions” and “carbon neutrality”.



The production process of bioethanol using lignocellulosic materials is dependent on three main steps including pretreatment, enzymatic hydrolysis and fermentation. Among them, enzymatic hydrolysis is the crucial step to convert polysaccharide in lignocellulosic material into glucose. There are many factors contribute to the recalcitrance of lignocellulosic material to hydrolysis, such as cellulase and its species, hydrolysis conditions, the crystallinity of cellulose, the accessibility of enzyme to cellulose, protection of cellulose by lignin [3–5]. Lignocellulosic material is a complex macromolecular material composed of cellulose, hemicellulose and lignin [6], while lignin, the main chemical component of plant fiber materials is a three-dimensional polymer composed of three phenylpropane units of guaiacyl (G), syringyl (S) and *p*-hydroxyphenyl (H), connected by ether bond and carbon-carbon bond [7]. The ratio of G, S and H units differs in softwood, hardwood and grass species [8]. Softwood lignin is mainly composed of G structural units, hardwood lignin is polymerized by G-type and S-type monomers, while grass lignin contains G, S and H structural units [9].

It has been reported that the presence of lignin in the enzymatic hydrolysis of cellulose is mainly manifested in two aspects: steric obstruction and non-productive adsorption caused by the interaction with enzymes [10]. Lignin forms non-productive adsorption with cellulase through hydrophobicity, electrostatic action and hydrogen bonding [11]. In recent years, there have been many research on the effect of lignin on enzymatic hydrolysis of cellulose [12–14]. Cao et al. [15] found that the smaller S/G ratio, the larger the adsorption capacity will be, through studying the enzyme adsorption capacity on lignin isolated from masson pine, poplar and wheat straw, respectively. However contradictory results on the S/G ratio effects were also reported. In the adsorption experiment of cellulase onto lignin from untreated and pretreated lignocellulose, Li et al. [16] found that the S/G ratio of lignin showed a positive effect on the ability of adsorbing enzymes, indicating that lignin with a high S/G ratio had a negative effect on enzymatic hydrolysis. Nonetheless, due to the complexity of lignin structure, the mechanism of lignin-enzyme interaction is still not clear. The purpose of this experiment is to study the dynamic behavior of lignin with different structural unit ratios, as well as cellulose complexes in enzyme adsorption and enzymatic hydrolysis, deeply understand the influence of single factors of lignin, and construct the structure-activity relationship between lignin structural units and cellulase adsorption and enzymatic hydrolysis sugar conversion. The milled wood lignin (MWL) samples with different structural units were extracted from three hardwoods. Quartz crystal microbalance (QCM) was used to explore the effects of different structural units of lignin on cellulase adsorption, and the data were fitted to establish a kinetic model, and further elucidate the effects of lignin on cellulase hydrolysis (The experimental method is shown in Fig. 1).

2 Materials and Methods

2.1 Materials

Poplar (*Populus deltoids*) was originally from Jiangsu OJI Paper Co., Ltd. (China), and eucalyptus (*Nitens*) and acacia (*Acacia mearnsii*) were both from Asia Symbol (Shandong) Pulp And Paper Co., Ltd. (China). The wood powder was grinded by Wiley micro mill. 40–80 mesh wood flour was screened, and extracted with benzene alcohol (2:1, v/v) for 8 h. The main chemical compositions of poplar, eucalyptus and acacia were shown in Table 1.

The cellulase (Cellic® CTec2) used in the experiment was purchased from Novozymes (Franklinton, NC, USA), and the cellulase filter paper activity was 200 FPU/g. The other chemicals were analytical grade and purchased from Sinopharmaceutical Chemical Reagents Co. Ltd. (China).

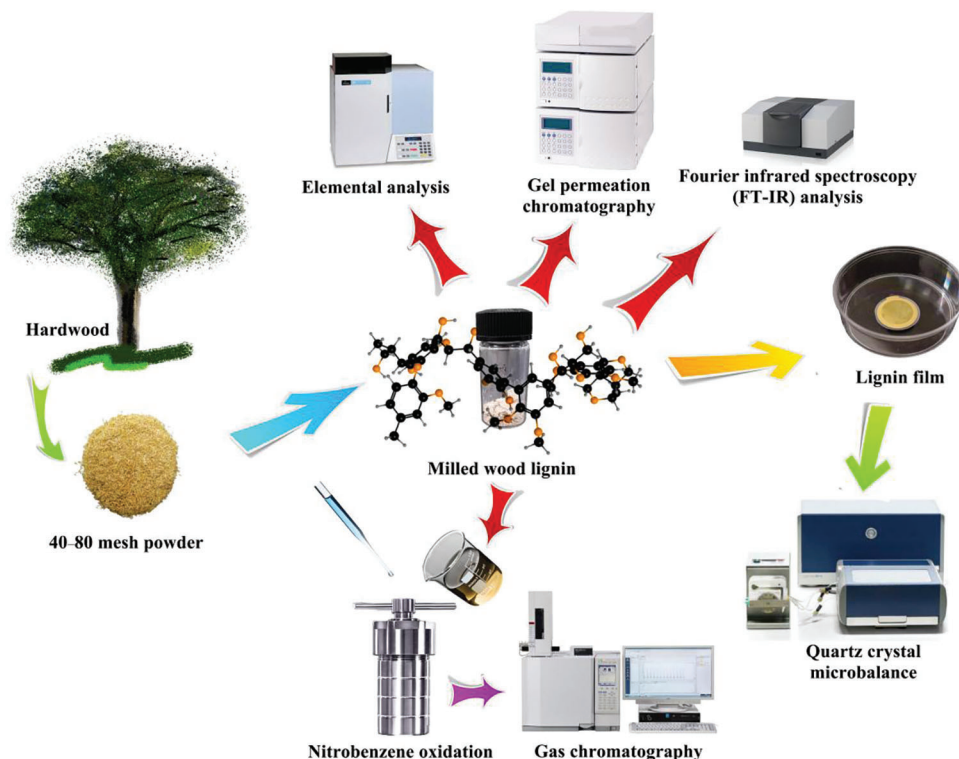


Figure 1: The steps of studying the interaction mechanism between lignin and enzyme

Table 1: The components of untreated materials

Materials	Lignin (% w/w)			Polysaccharide (% w/w)			
	Acid-insoluble lignin	Acid-soluble lignin	Total lignin	Glucan	Xylan	Araban	Total sugar
Poplar	22.85 ± 0.90	2.28 ± 0.56	25.13 ± 0.34	47.07 ± 0.63	22.95 ± 0.04	1.42 ± 0.28	71.44 ± 0.38
Eucalyptus	21.36 ± 0.11	3.89 ± 0.02	25.25 ± 0.09	46.80 ± 0.85	22.37 ± 0.32	3.64 ± 0.94	72.80 ± 0.41
Acacia	22.68 ± 0.86	3.02 ± 0.09	25.69 ± 0.76	45.27 ± 0.28	24.25 ± 0.23	3.97 ± 0.10	73.49 ± 0.40

2.2 Enzymatic Hydrolysis

Enzymatic hydrolysis was carried out at 50°C and 180 r/min in acetic acid-sodium acetate buffer (pH = 4.8) with 5% dry matter (w/v), and enzyme dosage of 30 FPU/g-cellulose. Samples were taken at regular intervals, and the concentration of monosaccharides in the hydrolysate was quantitated by high performance liquid chromatograph (Waters 1525, USA). The free protein in supernatant was determined by Bradford method using bovine serum albumin as the protein standard [17]. The conversion rate of glucan was calculated by the following formula, where Y was glucan conversion, %; c was the concentration of glucose in hydrolysate, g/L; 0.04 was the hydrolysate volume of the total hydrolysis system, L; 0.9 was the glucan conversion coefficient, m was raw material quality, g; w was the content of glucan in the raw material, %.

$$Y = (c \times 0.04 \times 0.9) / (m \times w) \times 100\% \quad (1)$$

2.3 Lignin Preparation

The degreased wood meal was ball milled in a miniature planetary ball mill (Fritsch GMBH, Germany) for 2 h at a fixed frequency of 600 r/min. Four grams of the sample (dry weight) was put into a silicon nitride ball milling tank with 25 zirconia balls (1 cm in diameter) in each. The ball milling was conducted at room temperature, and a 10 min operating break was provided after every 5 min of milling to avoid overheating.

Milled wood lignin was isolated based on the Björkman method [18,19]. The ball-milled wood powder was mixed with 96% dioxane with a solid-liquid ratio of 1:10 (w/v), and extracted with magnetic stirring for 48 h at room temperature. The supernatant was collected by centrifugation, the residue was continued to extract using the same method. The extracting solution collected twice was concentrated by rotary evaporation at 40°C to remove the solvent. The dried residue was dissolved in 90% (w/w) acetic acid, centrifugation, and the supernatant was introduced into water (10 times the volume of deionized water). The precipitated residue was subject to centrifugation, washing with water and freeze-drying. The crude lignin obtained was then sufficiently dissolved in a mixture of 1, 2-dichloroethane/ethanol (2:1, v/v) and centrifuged. The supernatant was added to a large amount of anhydrous ether, and the precipitate was washed with ether for three times to obtain lignin with high purity.

2.4 Acetylation of Lignin

Acetylation was carried out for determination of GPC according to the method of Gonzalo et al. [20]. The lignin (about 30 mg) was dissolved in 1.5 mL of pyridine-acetic anhydride mixture (1:2, v/v), and stirred at room temperature for 24 h without light. After the reaction, the reaction system was evaporated to dryness with absolute ethanol. Add 1 mL of chloroform to completely dissolve and drop into 100 mL of ether to precipitate acetylated lignin. The precipitate was washed several times with diethyl ether, and then put it into a 40°C-vacuum drying oven for drying.

2.5 Preparation of Lignin Films

The lignin was dissolved 8 wt% LiCl/DMSO at a concentration of 0.25%(w/w), and the prepared solutions were coated on the QCM gold sensors by spin coating method. The specific parameters were set as follows: spin coating at the speed of 5000 r/min for 3 times (dosage: 100 μ L each time), each time lasting for 1 min. The films were dried in an oven at 60°C, and immersed into ultra-pure water to remove LiCl and DMSO. The surface of the films then was dried with nitrogen gas and put in a dryer for later use.

2.6 Analytical Methods

2.6.1 Composition Analysis

The lignin and polysaccharide content of raw materials and MWL were analyzed according to an NREL protocol [21]. The samples were swollen with 72% H₂SO₄ at room temperature with occasional stirring for 3 h. After concentrated acid treatment, the mixture was diluted to 4% H₂SO₄ using distilled water, and reacted at 121°C for 1.5 h in an autoclave. The content of acid-insoluble lignin depended on hydrolysis residue, and the hydrolysate was used to determine the content of acid soluble lignin and sugar, respectively. The sum of acid-soluble lignin and acid-insoluble lignin was reported as the total lignin content. Acid soluble lignin was determined by calculating the absorbance at 205 nm in an UV-Vis spectrometer (TU-1900, China). The calculation of polysaccharide was based on the reference [22], and the content of polysaccharide was measured with a high-performance liquid chromatography (HPLC, Waters 1525, USA).

2.6.2 Crystallinity of the Raw Material

The crystallinity of the raw materials was analyzed by powder method on X-ray diffractometer (XRD, Ultima IV, Japan). Crystallinity can be calculated according to Segal formula [23], as shown below, where

I_{200} represented the peak intensity at $2\theta = 20^\circ\text{--}25^\circ$, and I_{am} represented the minimum peak intensity at $2\theta = 16^\circ\text{--}18^\circ$.

$$CrI(\%) = \frac{I_{200} - I_{am}}{I_{200}} \times 100\% \quad (2)$$

2.6.3 Elemental Analysis

The lignin samples of 2–3 mg were sealed in tin capsules, and elemental analyzer (PE 2400II, USA) was used for analyzing the elemental composition of C, H and O.

2.6.4 Gel Permeation Chromatography

The molecular weight and molecular distribution of lignin samples were determined by gel permeation chromatography (LC-20A, SHIMADZU, Japan) using tetrahydrofuran as the mobile phase at a flow rate of 1 mL/min.

2.6.5 Fourier Infrared Spectroscopy (FT-IR) Analysis

FT-IR analysis (VERTEX 80 V, Bruker, Germany) was carried out by potassium bromide wafer technique. The spectra were recorded in the $4000\text{--}400\text{ cm}^{-1}$ at a resolution of 4 cm^{-1} , and scanning time was 60 times/s.

2.6.6 Nitrobenzene Oxidation

Operation of nitrobenzene oxidation referred to the procedure reported by Chen [24]. The absolute-dried lignin samples (10 mg) were reacted with 4 mL sodium hydroxide (2 M NaOH) and 0.25 mL nitrobenzene in the stainless reaction bomb at 170°C for 2 h. At the end of the reaction, the tanks were placed in an ice water for rapid cooling, and 1 mL of internal standard (0.3 g/L 3-ethoxy-*p*-hydroxy benzaldehyde) was added. The mixture was extracted with dichloromethane (CH_2Cl_2) for three times with the dosage of 15 mL each time, and the water phase was collected. Hydrochloric acid (4 M HCl) was used to acidify the water phase layer to $\text{pH} = 1$. The acidified solution was extracted twice with CH_2Cl_2 (dosage: 20 mL each time), and the organic phase was collected. Then extracted with 15 mL diethyl ether and removed the water phase. The organic phase collected, and 20 mL distilled water was poured into the separation funnel, and the water phase was discarded. The remaining organic phase was dried by anhydrous sodium sulfite and evaporated to dry by rotary evaporation at 40°C . The dried product was dissolved with 1–2 mL ethyl ether, and 0.2 mL BSA (N, O-bis (trimethylsilyl) acetamide) was added. The derivatization conducted in an oven at 105°C for 10 min, and was analyzed by gas chromatograph (GC 2010PLUS, Shimadzu, Japan).

2.6.7 Enzyme-Lignin Surface Interaction Studied by QCM

The lignin films were loaded into the QCM module. The temperature was set at 40°C , and acetic acid-sodium acetate buffer ($\text{pH} 4.8$) was introduced into the module at a rate of 0.1 mL/min until the frequency vibration demonstrated a stable baseline. At the moment, cellulase solution with a concentration of 0.1 mg/mL was added and stopped 30 min later. After adsorption, buffer solution was added into the module again and rinsed for 15 min. Each experiment was measured at least 3 times, and the average of the 3 times was selected as the frequency. The fundamental frequency of all frequency variations was 5 MHz, and the overtones of 15, 25, 35 and 45 MHz were monitored simultaneously. The data in the third overtone (15 MHz) was selected for data processing.

3 Results and Discussion

3.1 Chemical Composition

The main chemical components of the three kinds of lignin were shown in Table 2. The MWL samples contained 0.08%–0.24% (w/w) of polysaccharide and the cellulose content only accounted for about 0.1%,

which meant that lignin can be used as an independent factor to study the effects on enzymatic hydrolysis regardless of the impact of carbohydrates in lignin samples.

Table 2: Chemical compositions of MWLs

Materials	Lignin (% w/w)			Polysaccharide (% w/w)		
	Acid-insoluble	Acid-soluble	Total lignin	Glucan	Xylan	Total sugar
Poplar MWL	87.67 ± 0.87	2.04 ± 0.32	89.70 ± 0.04	0.04 ± 0.02	0.04 ± 0.04	0.08 ± 0.01
Eucalyptus MWL	84.72 ± 0.43	4.36 ± 0.02	89.07 ± 0.12	0.07 ± 0.05	0.06 ± 0.02	0.13 ± 0.03
Acacia MWL	89.63 ± 0.67	1.96 ± 0.45	91.60 ± 0.54	0.12 ± 0.02	0.12 ± 0.02	0.24 ± 0.05

On the basis of the results of elemental analysis of poplar, eucalyptus and acacia MWL (Table 3), the contents of C, H and O of the three kinds of MWLs were close to each other, about 60% for C, 6% for H and 33% for O, respectively. Follow the C₉ molecular formula, the milled wood lignin of poplar, eucalyptus and acacia could be written as C₉H_{11.73}O_{4.75}, C₉H_{10.54}O_{4.35}, C₉H_{10.89}O_{3.89}.

Table 3: Element analysis of MWLs

Sample	Elemental composition (%)		
	C	H	O
Poplar MWL	56.83	6.18	39.99
Eucalyptus MWL	57.38	5.60	37.08
Acacia MWL	59.59	6.01	34.40

The number-average molecular weight (Mn), weight-average molecular weight (Mw) and polydispersity (Mw/Mn) of the three lignin samples were shown in Fig. 2. The molecular weight of the isolated MWL of poplar was 5232, similar to that of eucalyptus, 5402 and acacia, 5396. In addition, the Fig. 2 also showed the similar polydispersity, indicating that the molecular weight distribution of the extracted lignin was narrow and had good uniformity [25]. This observation indicated that the steric structure of the three kinds of lignin had little difference, and they had the similar steric hindrances induced in enzymatic hydrolysis.

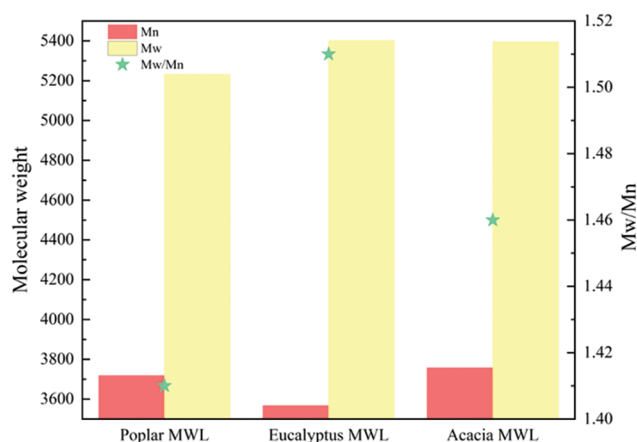


Figure 2: Molecular weight and polydispersity of MWLs

3.2 Nitrobenzene Oxidation Products

Alkaline nitrobenzene oxidation (NBO) is usually used to elucidation the structural analysis of lignin [26]. It could provide information about the constitutive monomeric composition of the lignin. After the reaction of lignin with nitrobenzene in alkaline conditions, the side chains of uncondensed lignin are oxidized by nitrobenzene, but the characteristics of the benzene ring in lignin are still retained [27]. The non-condensed guaiacyl, syringyl, and *p*-hydroxyphenyl groups are oxidized to aldehydes and to a lesser extent acids, and the yield of nitrobenzene oxidation products can reflect the degree of condensation of the reactants [28]. Products yields of alkaline nitrobenzene oxidation of isolated lignin samples were given in the Table 4.

Table 4: The alkaline nitrobenzene oxidation products yield of MWLs

Sample	Total nitrobenzene oxidation products yield (mmol/g lig)				S/G
	H	G	S	H+G+S	
Poplar MWL	0.02 ± 0.00	1.49 ± 0.02	1.47 ± 0.03	2.98 ± 0.05	0.99 ± 0.01
Eucalyptus MWL	0.02 ± 0.00	0.79 ± 0.03	1.52 ± 0.08	2.33 ± 0.11	1.92 ± 0.06
Acacia MWL	0.04 ± 0.00	1.13 ± 0.09	1.51 ± 0.04	2.68 ± 0.13	1.34 ± 0.01

Note: H is the sum of *p*-hydroxybenzaldehyde and *p*-hydroxybenzoic acid content; G is the sum of vanillin and vanillic acid contents; S is the sum of syringaldehyde and syringic acid content.

Obviously, the three lignin samples all produced a large amount of syringaldehyde/acid, vanillin/acid and a small amount of *p*-hydroxy benzoaldehyde/acid after nitrobenzene oxidation, which were typical hardwood lignin. Although they belong to the broad-leaved wood class, the lignin of eucalyptus, poplar and acacia showed their own distinct characteristics in chemical structure. The content of G units in eucalyptus lignin was only half of that of poplar lignin, which was much lower than that of poplar and acacia lignin. The S/G ratio of lignin in eucalyptus was 1.92, which was close to the oxidation results of nitrobenzene in eucalyptus by Xie et al. [29]. The S/G of poplar lignin was about 1, and that of acacia lignin was 1.34. The high content of uncondensed units in the lignin structure was indicative of the low degree of lignin condensation [30]. The total oxidation products yield of lignin in poplar, eucalyptus and acacia were 2.98, 2.33 and 2.68 mmol/g lig, respectively. The degree of lignin condensation in poplar was the least, followed by acacia and eucalyptus lignin.

3.3 FT-IR Analysis

The functional groups and bonds of isolated lignin samples were analyzed by FTIR spectroscopy (Fig. 3), and band assignments were based on data from the literature [31]. The main peaks ranged from 2000 cm⁻¹ to 800 cm⁻¹, and their relative peak intensities were listed in Table 5. Obviously, they had the similar structural skeletons, and the bands at 1594, 1505, and 1422 cm⁻¹ were attributed to aromatic ring vibration, indicating that the benzene ring structure of isolated lignin was intact. The C-H deformation vibrations on methyl and methylene were observed at 1462 cm⁻¹, and 836 cm⁻¹ represented the stretching vibration outside the C-H plane. The absorption bands at 1328, 1226 and 1125 cm⁻¹ were due to the vibration of the syringyl ring, while the relative band at 1270 cm⁻¹ represented the stretching vibration of the guaiacyl ring, which suggested that the three lignin samples all contain the S and G subunits. The absorption strength of lignin in eucalyptus was weak at 1270 cm⁻¹, due to the small number of G structural units, which was consistent with the results of alkaline nitrobenzene oxidation.

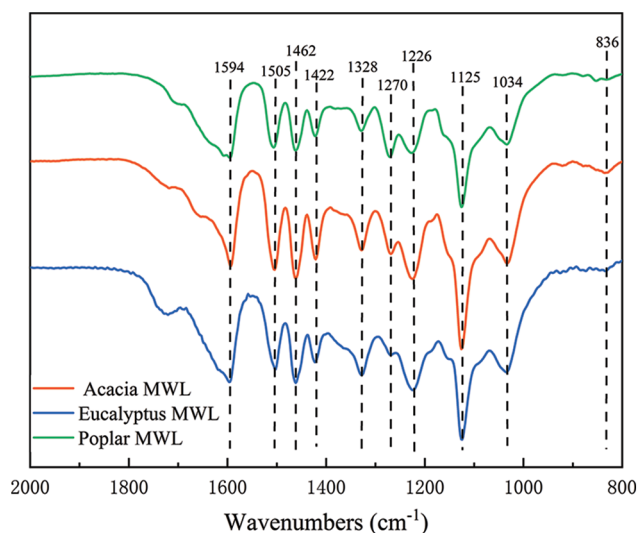


Figure 3: FT-IR spectra of MWLs

Table 5: Band assignments for the FT-IR spectra of MWLs

Wavenumber (cm ⁻¹)	Assignment
1594, 1505, 1422	Aromatic ring vibration
1462	C-H deformation vibrations on methyl and methylene
1328, 1226	Vibration of the syringyl ring
1270	Vibration of the guaiacyl ring
1125	C-OH stretching vibration
1034	C-O-C stretching vibration
836	Stretching vibration outside the C-H plane

3.4 Enzymatic Hydrolysis

Using the raw materials after ball milling of poplar, eucalyptus and acacia wood as substrate, enzymatic hydrolysis was carried out at 50°C and 180 r/min in acetic acid-sodium acetate buffer (pH 4.8). The change of glucan conversion rate over time was shown in Fig. 4. According to the analysis results of the three raw materials (Table 1), although the content of cellulose and lignin in poplar, eucalyptus and acacia was almost the same, the glucan conversion rates of the three feedstocks were different after 72 h hydrolysis. The sugar conversion rate of poplar was 68.02%, and that of eucalyptus was 66.50%, while the glucan conversion rate of acacia was much lower than that of poplar and eucalyptus wood, which was only 54.03%. In combination with the X-ray diffraction patterns and crystallinity of enzymatic hydrolysis raw materials in Fig. 5 and Table 6, the three hardwood raw materials have similar crystallinity. In theory, poplar, eucalyptus and acacia also have similar glucan conversion rates. However, the glucan conversion rate of acacia was much lower than that of poplar and Eucalyptus. This might be due to the difference in lignin structure in the substrate, which produces different results in the process of cellulase hydrolysis.

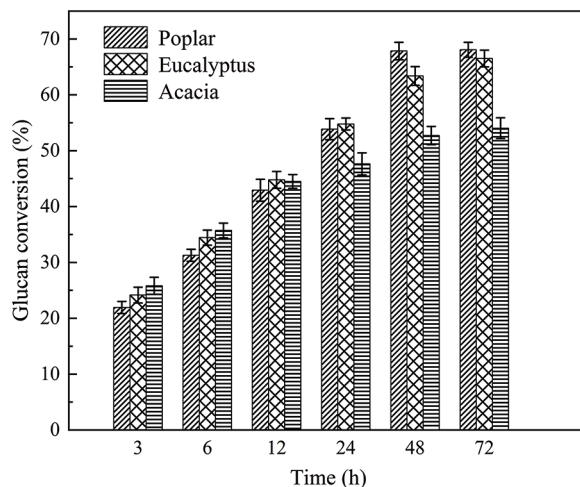


Figure 4: Glucan conversion of Poplar, Eucalyptus and Acacia

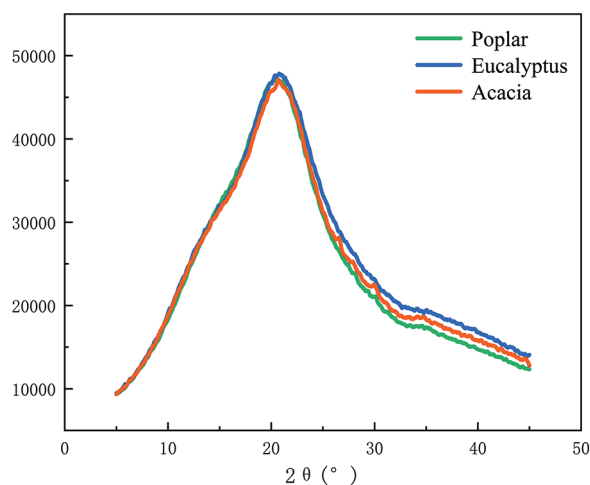


Figure 5: XRD spectra of untreated materials

Table 6: The crystallinity of untreated materials

Sample	I ₂₀₀	I _{am}	CrI (%)
Poplar	47259	34246	27.53
Eucalyptus	47853	33878	29.20
Acacia	47037	33320	29.16

The protein content detected in the supernatant was shown in Fig. 6. With the extension of hydrolysis time, the protein content in the supernatant first decreased, then increased, and then decreased slowly. In the initial stage of hydrolysis, a large number of cellulases were adsorbed on the hydrolysis substrate. With the progress of enzymatic hydrolysis reaction, more and more cellulose was hydrolyzed into glucose, more and more lignin was exposed, and some enzymes were slowly released into the supernatant [32], resulting in the increase of protein content in the supernatant. A small amount of cellulase will have ineffective adsorption with lignin, so the protein content in the supernatant will gradually decrease. The presence of lignin hinders the desorption of cellulase from the substrate [33]. Accordingly, in the initial stage of enzymatic hydrolysis,

compared with eucalyptus and acacia, the protein content of supernatant in poplar hydrolysate was the highest, and the content of cellulase adsorbed on poplar substrate was relatively low, and this part of enzyme adsorbed on substrate might adsorb with cellulose or non-productive adsorption with lignin.

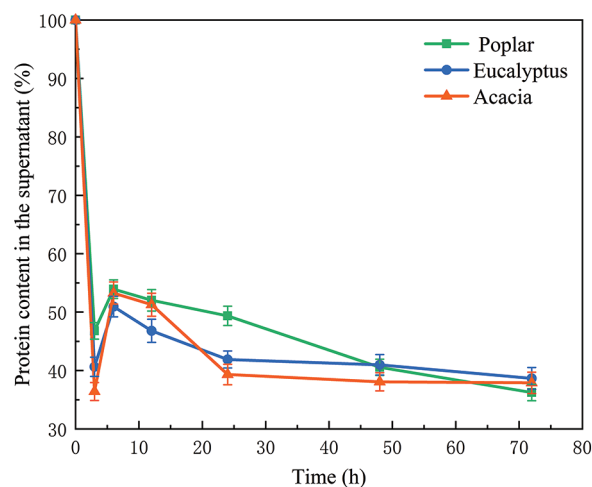


Figure 6: Protein content in the supernatant of Poplar, Eucalyptus and Acacia

3.5 Adsorption of Cellulase on Lignin

In order to determine whether the structure of lignin was the critical factor affecting the efficiency of enzymatic hydrolysis, the interaction between lignin and enzymes was studied *in situ* and in real time by preparing lignin films and using quartz crystal microbalance. Frequency changes of cellulase on lignin films of poplar, eucalyptus and acacia MWL were shown in Fig. 7. Since the frequency change of QCM was inversely proportional to the mass change of the film [34], the adsorption amount of cellulase on the lignin films could be intuitively seen through the frequency change. Once the frequency was in a stable state, the enzyme solution was introduced, and the frequency decreased instantaneously, indicating that the mass on the lignin film was increasing continuously, and the cellulase was rapidly adsorbing lignin. The decreasing rate of frequency reached a flat period after about 10 min, suggested that the adsorption rate of lignin by cellulase was slowing down. The frequency increased when the lignin film was rinsed with buffer solution, showing that a small part of the cellulase adsorbed on the lignin film was desorbed, but most of the cellulase was still tightly adsorbed with the lignin and was difficult to be eluted.

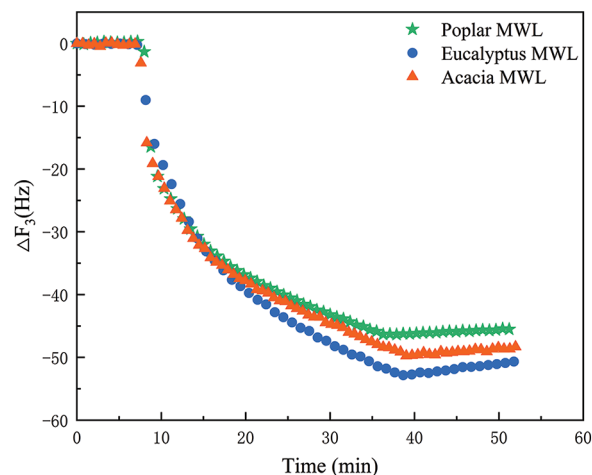


Figure 7: Adsorption of cellulase on lignin films

The difference of lignin structural units had a significant effect on the process of cellulase hydrolysis [35]. Compared to the maximum frequency of cellulase adsorption on lignin film in Fig. 7, it could be found that the adsorption capacity of cellulase on MWLs were in the following order: eucalyptus MWL > acacia MWL > poplar MWL. Combined with nitrobenzene oxidation results (The S/G ratios of poplar, eucalyptus and acacia MWL were 0.99, 1.92 and 1.34, respectively), the higher the S/G ratio of lignin, the stronger the enzyme adsorption capacity of lignin was, which reduced the contact opportunity of cellulose on the enzyme, and further blocked the accessibility between cellulose and enzymes, and finally retard the enzymatic efficiency. Tan et al. [36] also found in their study that sulfite pretreated lignin with high S/G ratio had stronger adsorption capacity than untreated lignin. Compared with the G structural unit, S unit showed a higher affinity for cellulase and induced more enzymes to adsorb on the lignin films irreversibly. In addition, the structure of S unit contained two methoxy groups, which caused the more space obstacles [37], thus hindering the adsorption of enzymes to cellulose. Beyond that, the contents of non-condensed units in MWL of poplar, eucalyptus and acacia were 2.98, 2.33 and 2.68 mmol/g lig. The adsorption amount of cellulase was also related to the condensation degree of lignin. The greater the degree of condensation, the stronger the interaction between lignin and enzymes was [38].

Frequency data obtained by QCM could also be combined with the exponential attenuation model (3) to establish the adsorption kinetics equation of lignin and enzyme [39]. Since the frequency (ΔF) and the mass (Δm) of the enzyme adsorbed on the surface of lignin films also accorded with the Sauerbrey linear formula (4) [40], the maximum adsorption amount and irreversible adsorption amount of cellulase on different lignin films could be calculated.

$$\Delta F = \Delta F_{\max} \left(1 - e^{-\frac{t}{\tau}}\right) \quad (3)$$

$$\Delta m = \frac{-c\Delta F}{n} \quad (4)$$

In formula (3), ΔF_{\max} was the frequency when the maximum adsorption capacity was reached, Hz; t is time, min; τ was the reciprocal of adsorption rate, min^{-1} . In formula (4), Δm was the adsorption mass, ng/cm^2 ; c was the mass sensitivity constant, where $c = 17.7 \text{ ng}/\text{cm}^2/\text{Hz}$; ΔF was the frequency, Hz; n was the octave value, $n = 3, 5, 7, 9, 11$ ($n = 3$, in this work).

The fitting results of cellulase adsorption kinetics on lignin were shown in Table 7, and the fitting correlation coefficients were all greater than 0.9. The adsorption rate, maximum adsorption amount and irreversible adsorption amount of different lignin films were different. Among them, the adsorption rate of cellulase on poplar MWL was the highest, followed by acacia MWL, and eucalyptus MWL. On the grounds of the maximum adsorption amount and irreversible adsorption amount, the desorption capacity of cellulase on poplar, eucalyptus and acacia lignin films was 45.7, 72.0 and 47.4 ng/cm^2 , respectively, showing that the adsorption layer formed by cellulase on MWL film of eucalyptus was the most loose, which made it easier to desorption from lignin substrate. However, because of the higher S/G ratio of eucalyptus MWL, there were more sites that can be adsorbed with cellulase, which made the stronger adsorption capacity of eucalyptus and cellulase and the larger irreversible adsorption amount larger. This result was consistent with previous work [41,42].

Table 7: Adsorption parameters of cellulase on lignin films

Film sample	$-\Delta F_{\max}$ (Hz)	$1/\tau$ (min^{-1})	R^2	Maximum adsorption amount (ng/cm^2)	Irreversible adsorption amount (ng/cm^2)
Poplar MWL	53.32	0.051	0.908	314.6	268.9
Eucalyptus MWL	62.59	0.043	0.927	369.4	297.4
Acacia MWL	56.51	0.049	0.929	333.4	286.0

4 Conclusion

Using poplar, eucalyptus and acacia wood as raw materials, milled wood lignin was extracted by Bjökman method. With detailed comparison of lignin structures, there was no significant difference between the three lignin samples, except for differences in lignin structural units. In the hydrolysis experiment, the results of enzymatic hydrolysis kinetic parameters based on QCM demonstrated that the lignin with higher S/G ratio showed a stronger affinity for cellulase, which caused more enzyme to be covered in the network structure of lignin. The more non-productive adsorption between lignin and enzyme with high S/G ratio will lead to the decrease of adsorption between enzyme and cellulose, resulting in a decrease in hydrolysis efficiency.

Funding Statement: National Natural Science Foundation of China (31730106, 21704045).

Conflicts of Interest: The authors declare that they have no conflicts of interest to report regarding the present study.

References

1. Devi, A., Singh, A., Bajar, S., Pant, D., Din, Z. U. (2021). Ethanol from lignocellulosic biomass: An in-depth analysis of pre-treatment methods, fermentation approaches and detoxification processes. *Journal of Environmental Chemical Engineering*, 9(5), 105798. DOI 10.1016/J.JECE.2021.105798.
2. Betül, G., Hakki, G., Emir, Z. H. (2021). Bioethanol production from pistachio (*pistacia vera* L.) shells applying ozone pretreatment and subsequent enzymatic hydrolysis. *Environmental Technology*, 42(15), 2438–2446. DOI 10.1080/09593330.2021.1903565.
3. Cheng, L., Hu, X. H., Gu, Z. B., Hong, Y., Li, Z. F. et al. (2019). Characterization of physicochemical properties of cellulose from potato pulp and their effects on enzymatic hydrolysis by cellulase. *International Journal of Biological Macromolecules*, 131, 564–571. DOI 10.1016/j.ijbiomac.2019.02.164.
4. Yuan, Y. F., Jiang, B., Chen, H., Wu, W. J., Wu, S. F. et al. (2021). Recent advances in understanding the effects of lignin structural characteristics on enzymatic hydrolysis. *Biotechnology for Biofuels*, 14(1), 205. DOI 10.1186/S13068-021-02054-1.
5. Satari, B., Karimi, K., Molaverdi, M. (2018). Structural features influential to enzymatic hydrolysis of cellulose-solvent-based pretreated pinewood and elmwood for ethanol production. *Bioprocess and Biosystems Engineering*, 41(2), 249–264. DOI 10.1007/s00449-017-1863-2.
6. Mou, H. Y., Liu, Y. B., Huang, J. (2020). Adsorption effects of lignin on different enzyme proteins. *Transactions of China Pulp and Paper*, 35(4), 23–2. DOI 10.11981/j.issn.1000-6842.2020.04.23.
7. Zhang, H. Y., Chen, T., Li, Y., Han, Y., Sun, Y. N. et al. (2020). Novel lignin-containing high-performance adhesive for extreme environment. *International Journal of Biological Macromolecules*, 164, 1832–1839. DOI 10.1016/j.ijbiomac.2020.07.307.
8. Zhu, Y. K., Huang, J. W., Wang, K. L., Wang, B., Sun, S. L. et al. (2020). Characterization of lignin structures in *phyllostachys edulis* (Moso bamboo) at different ages. *Polymers*, 12(1), 187. DOI 10.3390/polym12010187.
9. Sheng, Y. Q., Shiung, L. S., Wu, Y. J., Ge, S. B., Wu, J. L. et al. (2020). Enzymatic conversion of pretreated lignocellulosic biomass: A review on influence of structural changes of lignin. *Bioresource Technology*, 324, 124631. DOI 10.1016/J.BIORTECH.2020.124631.
10. An, S. X., Li, W. Z., Xue, F. Y., Xu, L., Ying, X. et al. (2020). Effect of removing hemicellulose and lignin synchronously under mild conditions on enzymatic hydrolysis of corn stover. *Fuel Processing Technology*, 204, 106407. DOI 10.1016/j.fuproc.2020.106407.
11. Li, M. H., Yuan, Y. F., Zhu, Y. S., Jiang, B., Wu, W. J. et al. (2021). Comparison of sulfomethylated lignin from poplar and masson pine on cellulase adsorption and the enzymatic hydrolysis of wheat straw. *Bioresource Technology*, 343, 126142. DOI 10.1016/J.BIORTECH.2021.126142.

12. Zheng, W. Q., Lan, T. Q., Li, H., Yue, G. J., Zhou, H. F. et al. (2020). Exploring why sodium lignosulfonate influenced enzymatic hydrolysis efficiency of cellulose from the perspective of substrate-enzyme adsorption. *Biotechnology for Biofuels*, 13, 19. DOI 10.1186/s13068-020-1659-5.
13. Kim, J. E., Lee, J. W. (2018). Enzyme adsorption properties on dilute acid pretreated biomass by low vacuum-scanning electron microscopy and structural analysis of lignin. *Bioresource Technology*, 262, 107–113. DOI 10.1016/j.biortech.2018.04.068.
14. Chen, H., Jiang, B., Wu, W. J., Jin, Y. C. (2020). Comparison of enzymatic saccharification and lignin structure of masson pine and poplar pretreated by *p*-toluenesulfonic acid. *International Journal of Biological Macromolecules*, 151, 861–869. DOI 10.1016/j.ijbiomac.2020.02.242.
15. Cao, T. Y. (2018). *The effect of lignin structure on cellulase adsorption and enzymatic hydrolysis by using QCM*. Nanjing, China: Nanjing Forestry University.
16. Li, M. F., Yi, L., Bin, L., Zhang, Q. T., Song, J. L. et al. (2020). Comparison of nonproductive adsorption of cellulase onto lignin isolated from pretreated lignocellulose. *Cellulose*, 27(14), 7911–7927. DOI 10.1007/s10570-020-03357-6.
17. Bradford, M. M. (1976). A rapid and sensitive method for the quantitation of microgram quantities of protein utilizing the principle of protein-dye binding. *Analytical Biochemistry*, 72(1–2), 248–254. DOI 10.1016/0003-2697(76)90527-3.
18. Bjökman, A. (1957). Lignin and lignin-carbohydrate complexes extraction from wood meal with neutral solvents. *Industrial & Engineering Chemistry*, 49, 1395–1398. DOI 10.1021/ie50573a040.
19. Bjökman, A. (1956). Studies on finely divided wood (I) extraction of lignin with neutral solvents. *Svensk Papperstidn*, 59, 477–485.
20. Gonzalo, V., Sonia, F., Carlos, R. B., Julia, G., Gervasio, A. et al. (1999). Structures, and reactivities with formaldehyde, of some acetosolv pine lignins. *Journal of Wood Chemistry & Technology*, 19(4), 357–378. DOI 10.1080/02773819909349617.
21. Dence, C. W., Lin, S. Y. (1992). *Introduction in methods in lignin chemistry*. Heidelberg: Springer Verlag Press.
22. Borchardt, L. G., Piper, C. V. (1970). A gas chromatographic method for carbohydrates as alditol-acetates. *Tappi Journal*, 53, 257–260.
23. Segal, L., Creely, J. J., Martin, A. E., Conrad, C. M. (1959). An empirical method for estimating the degree of crystallinity of native cellulose using the X-ray diffractometer. *Textile Research Journal*, 29(10), 786–794. DOI 10.1177/004051755902901003.
24. Chen, C. L. (1992). Nitrobenzene and cupric oxide oxidations. In: Lin, S. Y., Dence, C. W. (Eds.), *Methods in lignin chemistry*. pp. 301–321. New York: Springer.
25. Yan, Z. Y., Wei, L. L., Deng, Y. J., Tian, Q. W., Fang, G. G. (2020). Fractionation and performance comparison of sulfate lignin. *Applied Chemical Industry*, 49(7), 1626–1629. DOI 10.16581/j.cnki.issn1671-3206.2020.07.002.
26. Min, D. Y., Xiang, Z. Y., Liu, J., Jameel, H., Chiang, V. et al. (2014). Improved protocol for alkaline nitrobenzene oxidation of woody and non-woody biomass. *Journal of Wood Chemistry and Technology*, 35(1), 52–61. DOI 10.1080/02773813.2014.902965.
27. Zhou, Q., Xu, M., Huang, H., Cao, Y. F., Liu, Z. L. (2020). Effects of dioxane aqueous solution on the regenerating of wheat straw solution and isolating efficiency of LCC. *Journal of Cellulose Science and Technology*, 28(3), 1–9. DOI 10.16561/j.cnki.xws.2020.03.05.
28. Chen, C. L. (1992). Nitrobenzene and cupric oxide oxidations. In: *Methods in lignin chemistry*. Berlin: Springer-Verlag.
29. Xie, Y. M., Wu, H., Lai, Y. M. (1998). Effect of chemical composition and wood property on kraft pulping of eucalyptus. *China Pulp & Paper*, 17(5), 7–11.
30. Xu, C., Zhang, J., Zhang, Y., Guo, Y., Xu, H. J. et al. (2019). Lignin prepared from different alkaline pretreated sugarcane bagasse and its effect on enzymatic hydrolysis. *International Journal of Biological Macromolecules*, 141, 484–492. DOI 10.1016/j.ijbiomac.2019.08.263.

31. Xu, C., Liu, F., Alam, M. A., Chen, H. J., Zhang, Y. et al. (2020). Comparative study on the properties of lignin isolated from different pretreated sugarcane bagasse and its inhibitory effects on enzymatic hydrolysis. *International Journal of Biological Macromolecules*, 146, 132–140. DOI 10.1016/j.ijbiomac.2019.12.270.
32. Nakagame, S. P., Chandra, R., Saddler, J. N. (2010). The effect of isolated lignins, obtained from a range of pretreated lignocellulosic substrates, on enzymatic hydrolysis. *Biotechnology and Bioengineering*, 105(5), 871–879. DOI 10.1002/bit.22626.
33. Tu, M. B., Chandra, R. P., Saddler, J. N. (2007). Evaluating the distribution of cellulases and the recycling of free cellulases during the hydrolysis of lignocellulosic substrates. *Biotechnology Progress*, 23(2), 398–406. DOI 10.1021/bp060354f.
34. He, J., Huang, C. X., Lai, C. H., Jin, Y. C., Ragauskas, A. et al. (2020). Investigation of the effect of lignin/pseudolignin on enzymatic hydrolysis by quartz crystal microbalance. *Industrial Crops and Products*, 157, 112927. DOI 10.1016/j.indcrop.2020.112927.
35. Li, X., Zheng, Y. (2017). Lignin-enzyme interaction: Mechanism, mitigation approach, modeling, and research prospects. *Biotechnology Advances*, 35(4), 466–489. DOI 10.1016/j.biotechadv.2017.03.010.
36. Tan, L. P., Sun, W., Li, X. Z., Zhao, J., Qu, Y. B. et al. (2015). Bisulfite pretreatment changes the structure and properties of oil palm empty fruit bunch to improve enzymatic hydrolysis and bioethanol production. *Biotechnology Journal*, 10(6), 915–925. DOI 10.1002/biot.201400733.
37. Santos, R. B., Lee, J. M., Jameel, H., Chang, H. M., Lucia, L. A. (2012). Effects of hardwood structural and chemical characteristics on enzymatic hydrolysis for biofuel production. *Bioresource Technology*, 110, 232–238. DOI 10.1016/j.biortech.2012.01.085.
38. Yu, Z. Y., Gwak, K. S., Treasure, T., Jameel, H., Chang, H. M. et al. (2014). Effect of lignin chemistry on the enzymatic hydrolysis of woody biomass. *ChemSusChem*, 7(7), 1942–1950. DOI 10.1002/cssc.201400042.
39. Lin, X. L., Wu, L. J., Huang, S. Q., Qin, Y. L., Qiu, X. Q. et al. (2019). Effect of lignin-based amphiphilic polymers on the cellulase adsorption and enzymatic hydrolysis kinetics of cellulose. *Carbohydrate Polymers*, 207, 52–58. DOI 10.1016/j.carbpol.2018.11.070.
40. Rodahl, M., Höök, F., Krozer, A., Brzezinski, P., Kasemo, B. (1995). Quartz crystal microbalance setup for frequency and Q-factor measurements in gaseous and liquid environments. *Review of Scientific Instruments*, 66(7), 3924–3930. DOI 10.1063/1.1145396.
41. Li, M., Si, S. L., Hao, B., Zha, Y., Wan, C. et al. (2014). Mild alkali-pretreatment effectively extracts guaiacyl-rich lignin for high lignocellulose digestibility coupled with largely diminishing yeast fermentation inhibitors in miscanthus. *Bioresource Technology*, 169, 447–454. DOI 10.1016/j.biortech.2014.07.017.
42. Min, D. Y., Yang, C. M., Shi, R., Jameel, H., Chiang, V. et al. (2013). The elucidation of the lignin structure effect on the cellulase-mediated saccharification by genetic engineering poplars (*Populus nigra* L. × *Populus Maximowiczii* A.). *Biomass and Bioenergy*, 58, 52–57. DOI 10.1016/j.biombioe.2013.08.019.